Young person's guide to translation surfaces of genus two: McMullen's Connected Sum Theorem.

Andrew Bouwman and Jaroslaw Kwapisz*

Department of Mathematical Sciences
Montana State University
Bozeman MT 59717-2400
http://www.math.montana.edu/~jarek/

August 3, 2012

Abstract

A translation surface is a surface obtained by identifying pairs of parallel edges of a polygon in the Cartesian plane $\mathbb{R}^2$. We give an introduction to translation surfaces of genus two including their hyperellipticity and a detailed elementary proof of McMullen's result that any such surface can be obtained as a connected sum of two flat tori.

1 Introduction

We give an introduction to some basic properties of translation surfaces of genus two, including their hyperellipticity and McMullen's theorem that any such surface can be obtained as a connected sum of two flat tori joined along a straight slit [6] (Figure 1). This decomposition result enabled McMullen to leverage the classical theory of genus one surfaces to obtain deep insight into the properties of the $\mathbb{SL}_2(\mathbb{R})$ action on the bundle of holomorphic one-forms in genus two. In particular, he classified the possible orbit closures establishing the analogues of Raghunathan's conjectures in this context.

Our goal is to make the decomposition theorem accessible to an uninitiated reader by supplying an alternative detailed argument proceeding through elementary geometric considerations. The proof offers a new perspective on the relative

*E-mail contact: abouwman@math.montana.edu, jarek@math.montana.edu

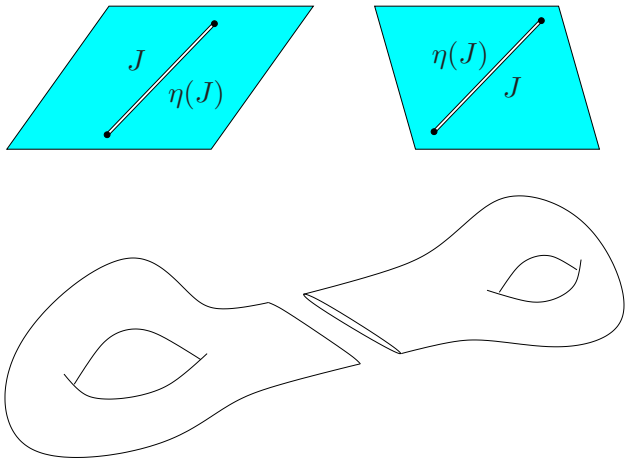

Figure 1: A genus two surface as a sum of two slitted tori. (The slits glue together to form a saddle connection J and its image $\eta(J)$ under the hyperelliptic involution η, which acts on the parallelograms by their central symmetry.)

combinatorial simplicity enjoyed by the case of genus two (as compared with higher genera).

Our departure point is an observation that there is only one combinatorial type of arc exchanges induced on a closed geodesic cross-section by the vertical flow on M. This is the content of Discrete Datum Theorem in Section 2, which also contains the necessary background on translation surfaces. This theorem offers an alternative to the classification of "ribbon graphs" relied on by McMullen. Section 3 gives some immediate corollaries showing, in particular, how one can avoid the more advanced tools of complex analysis to establish the hyperellipticity and existence of Weierstrass points on M. These play a pivotal role in McMullen's result, which is stated and demonstrated in Section 4.

Upon completion of this work, we learned that a similar proof of existence of splittings can be found in the survey [2] but the result there is weaker in that it gives *one* splitting whereas McMullen's theorem secures an infinite number (as required by the application to the $\mathbb{SL}_2(\mathbb{R})$ action).

2 Translation Surfaces and Polyband Construction

A translation surface M is a surface obtained by identifying the corresponding edges of a polygon P (contained in $\mathbb{R}^2$) whose edges come in pairs e^+ and e^- where e^- is a translation of e^+. Taking P to be a regular polygon gives nice examples, with the square and the hexagon yielding a torus and the octagon yielding a torus with one "handle" attached (a genus two surface, as in the inset in Figure 3). Figure 2 depicts a more "generic" octagon. The identifications being effected by

translations, M is locally isometric to $\mathbb{R}^2$ at all points with the possible exception of the vertices where a conical singularity may form with the total angle that is a multiple of 2π. Alternatively, a translation surface can be defined as a compact two dimensional (real) surface carrying on the complement of a finite set an atlas of charts into $\mathbb{R}^2$ whose transition functions are translations. To ensure that the omitted points are conical singularities it is furthermore assumed that the area of the surface is finite.

If one thinks of $\mathbb{R}^2$ as identified with the complex numbers $\mathbb{C}$ in the usual way, then the atlas determines a structure of a Riemann surface and also gives a holomorphic 1-form obtained by pulling back $dz = dx + idy$ via the charts. The process can be reversed[1] and, in complex analysis, translation surfaces are usually spoken of as holomorphic 1-forms on Riemann surfaces. That is the language of [6], but we will use it only briefly to illustrate (in Section 3) the utility of our approach. The interplay between different perspectives on translation surfaces make it an exciting and rich subject; see the surveys [5, 10] (or the source [3]).

Going back to the identified polygon, if the genus of M is to be $g = 2$, then we can either have one singularity with angle 6π or two singularities each with angle 4π. This can be seen by applying the Poincaré-Hopf formula to a vertical vector field on M or by computing the Euler characteristic of M from a partition of M into rectangles such that a vertex of any one of two touching rectangles is a vertex of both.[2] The subcollections of genus two translation surfaces with one 6π singularity or two 4π singularities are denoted $\mathcal{H}(2)$ and $\mathcal{H}(1,1)$, respectively.

Whether M is in $\mathcal{H}(2)$ or $\mathcal{H}(1,1)$ depends on the number of sides of P and the order in which they are arranged along its boundary. To neatly organize the possible orders, we introduce below a variation of the polygon construction where P comes with two sides "pre-glued" and thus forms a "band". (Theorem 1 ahead asserts that M is always obtainable in this way.)

Consider the strip $\mathcal{S} := \{(x, y) : \ 0 \le x \le 1\}$ and the infinite cylinder $\mathcal{S}/\!\sim$ in $\mathbb{R}^2$ obtained by identifying the boundary lines of $\mathcal{S}$ by the translation $(x, y) \mapsto (x+1, y)$. Let L^+ be a closed broken line (broken geodesic) in $\mathcal{S}/\!\sim$ that is a graph of a continuous function over the *equatorial circle* $E := \{(x, 0) : \ 0 \le x \le 1\}/\!\sim$ and consists of m ($m \ge 2$) segments (see Figure 2). Suppose that L^- in $\mathcal{S}/\!\sim$ is another broken line lying below E and obtained from L^+ by rearrangement of its segments by translations. The topological annulus $\mathcal{A}$ in $\mathcal{S}/\!\sim$ bounded by L^+ and

[1] This can be done by representing M via Veech's "zippered rectangle" [8] erected over the first return map of the geodesic flow in a minimal direction for the metric associated with the 1-form.

[2] To each vertex v associate $i(v) \in \mathbb{N}$ so that $i(v) \cdot 2\pi$ is the total angle at v making v a common point of $i(v) \cdot 4$ rectangles and $i(v) \cdot 4$ edges. The Euler characteristic $2 - 2g = -2$ is expressed as

$$V - E + F = \sum_v 1 - \frac{1}{2} \sum_v i(v) \cdot 4 + \frac{1}{4} \sum_v i(v) \cdot 4 = -2.$$

Hence, $\sum_v i(v) - 1 = 2$ yielding the two possibilities $2 = 2$ or $1 + 1 = 2$.

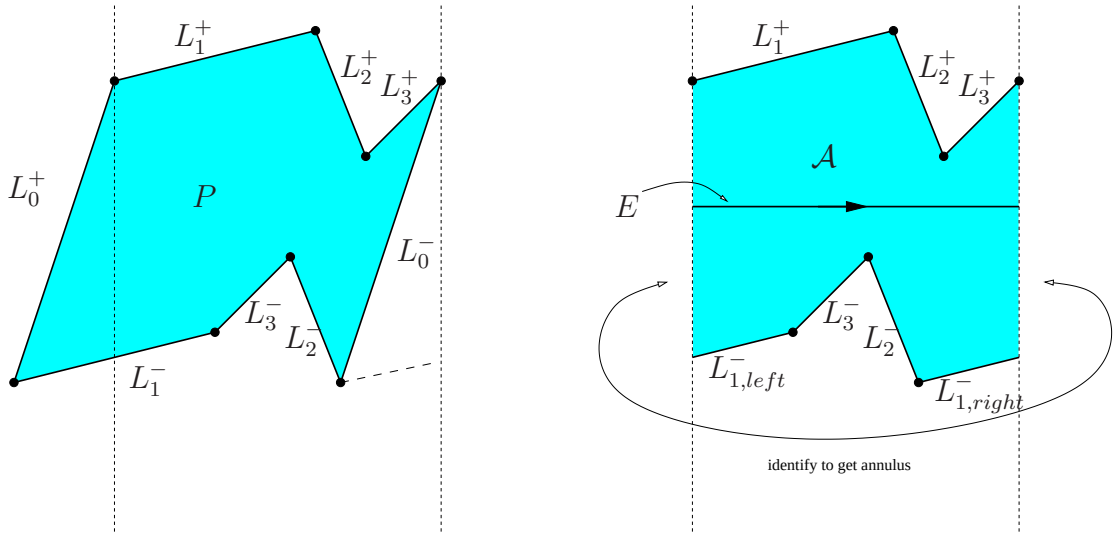

Figure 2: $M \in \mathcal{H}(2)$ arises from gluing sides of a polygon P (left) or a polyband $\mathcal{A}$ (right).

L^- forms a translation surface upon identifying the corresponding segments of L^+ and L^-. For lack of a better name, we call the *polygonal band* $\mathcal{A}$ a *polyband* and the whole process a *polyband construction*.

Each instance of the polyband construction can be assigned a *discrete datum* as follows. Give L^+ and L^- the orientation induced from the standard orientation on E by projecting. Label the edges of L^+ as $L_1^+, \ldots, L_m^+$ by going once around L^+ in the positive direction starting from some edge. Label the edges of L^- as $L_1^-, \ldots, L_m^-$ where the L_i^- is the segment corresponding to L_i^+ under the rearrangement that formed L^- from L^+. Going around L^- in the positive direction starting from some edge the encountered edges are $L_{\pi(1)}^-, \ldots, L_{\pi(m)}^-$ where π is a permutation of $\{1, \ldots, m\}$. In Figure 2, starting from L_3^-, the π is $(3, 2, 1)$, i.e., $\pi(1) = 3$, $\pi(2) = 2$, and $\pi(3) = 1$. This permutation depends on the choice of the starting edges on L^+ and L^- so, to remove this ambiguity, we consider two permutations π and π' as equivalent iff $\pi = c_1 \circ \pi' \circ c_2$ where the c_i are some powers of the cyclic permutation $(2, \ldots, m, 1)$. The equivalence class, called a *reduced permutation*, is what we brand as the *discrete datum* of the construction. We will denote it by using square brackets; in Figure 2 the discrete datum is $[3, 2, 1]$. (One can check that for $m = 3$ there are only two distinct reduced permutations: $[1, 2, 3]$ and $[3, 2, 1]$, while for $m = 4$ there are three: $[1, 2, 3, 4]$, $[4, 3, 1, 2]$, and $[4, 3, 2, 1]$.) The following result is our way of expressing the combinatorial simplicity of genus two translation surfaces.

Theorem 1 (Discrete Datum Theorem)**.** *(i) Any $M \in \mathcal{H}(2)$ is isometric to a translation surface obtained from a polyband construction with discrete datum $[3, 2, 1]$. (ii) Any $M \in \mathcal{H}(1, 1)$ is isometric to a translation surface obtained from a polyband*

construction with discrete datum [4, 3, 2, 1].

To prove the theorem, we use that any translation surface has a regular closed geodesic (i.e. a closed geodesic disjoint from the singular points). This innocent fact is not trivial and has been originally shown by Masur with help from Teichmüller theory [4]. A nice elementary proof has been found by Smillie [7] (see also [9]). The crux is in deforming P by an affine transformation so that M has area $A = 1$ and the diameter of M is so large that some point $p \in M$ is further than $1/\sqrt{\pi}$ from the singularities (see Figure 3)[3]. (Affine transformations map closed geodesics to closed geodesics.) Since $A = 1$, upon increasing $r > 0$ from zero, the r-neighborhood $B_r(p)$ in M centered at p must cease to be an embedded Euclidean disk for some $r_0 \in (0, 1/\sqrt{\pi}]$. For r that is a tad bigger than r_0, $B_r(p)$ is still free of singularities but "laps over itself" and thus contains a flat cylinder made of a multitude of parallel regular closed geodesics.

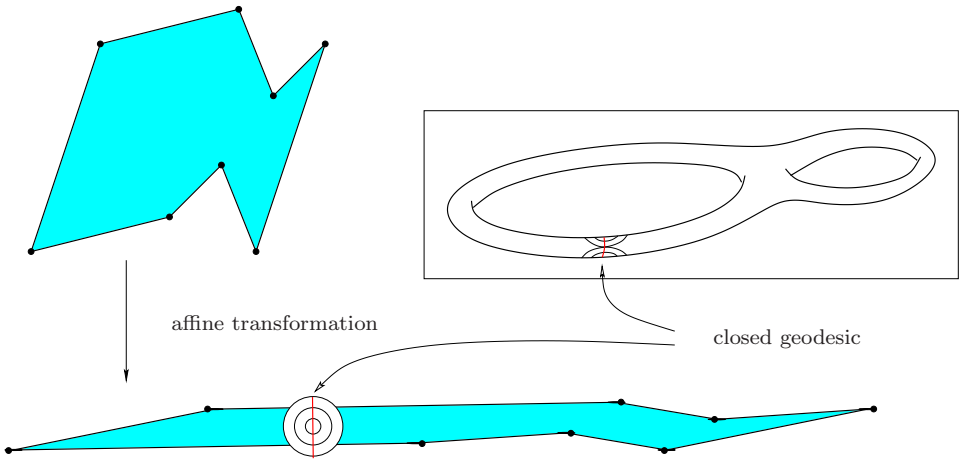

Figure 3: Smillie's construction of a (regular) closed geodesic.

As another standard preliminary, let us fix a regular closed geodesic E and some direction transversal to E. Consider the subset M' of the points p' of M that can be reached from a point of E by traveling along geodesic segments of that fixed direction. Here we do not insist that a single segment is used for any given point p' and allow unions of segments joined at singularities of M. It is not hard to see that, unless M' coincides with all of M, its boundary must be a union of *saddle connections*, that is geodesic segments connecting singularities. In particular, by choosing a *generic* direction, that is not one of the countably many directions of all possible saddle connections, one can ensure that $M' = M$.

Proof of Theorem 1: Consider a translation surface M of genus two. Let E be a regular closed geodesic. Pick a *generic* direction transversal to E as in our

[3]The delicate point is that the diameter of M is generally smaller than the diameter of the deformed P.

preliminary discussion so that $M' = M$ and every geodesic segment in the chosen direction contains at most one singularity. It is convenient to apply an affine transformation to make the direction vertical and E horizontal. Consider the first return map $T : E \to E$ under the *vertical flow*, i.e., the movement of points of M with unit speed in the vertical direction, which is unambiguously defined except at the singularities having several outgoing verticals. T is an *arc exchange*: it is a well defined local isometry apart from the finitely many points p whose outgoing vertical geodesic hits a singularity s before returning to E. T acts by cutting E at all such *cut points* p and rearranging the resulting arcs in E by translations. At this point we are tempted to say that T is *easily seen* to be as depicted in one of Figures 4 and 5, but let us flesh out this argument.

To be precise, for small $\epsilon > 0$, the horizontal arc $(p - \epsilon, p + \epsilon)$ centered at a cut point p flows vertically intact and sweeps a rectangle in M until it hits a singularity s where the rectangle is slit along two verticals outgoing from s and forming angle 2π in M. (By our choice of direction, the slitted rectangle has its two parts returning to E without further encounters with singularities, granted $\epsilon > 0$ is small enough.) In particular, a small portion of the slitted rectangle forms a small radius 2π-sector with a tip at s (darkly shaded in Figure 4). Such sectors for different p are disjoint and (their closures) form a neighborhood of the set of singularities. Therefore, if $M \in \mathcal{H}(2)$ then there are $6\pi/2\pi = 3$ cut points p in E and if $M \in \mathcal{H}(1,1)$ then there are $(4\pi + 4\pi)/2\pi = 4$ cut points.

Let us focus on the case $M \in \mathcal{H}(2)$ when E is cut into three (open) arcs E_1, E_2, E_3 (Figure 4). Each arc E_i sweeps an open rectangle R_i before returning to E. The vertical portions of the boundaries of any two adjacent rectangles $\overline{R}_i$ and $\overline{R}_{i+1}$ that are below the singularity impact are identified in M. We shall call the disjoint union $\mathcal{R}$ of $\overline{R}_1$, $\overline{R}_2$, and $\overline{R}_3$ with those identifications a *tower*. As discussed, the vertical sides of the tower (above the singularities) are identified so that M contains a neighborhood of s with the total angle at s equal to 6π. In Figure 4, the neighborhood is glued together from the three small darkly shaded slitted rectangles labeled by the three tower vertices s_{12}, s_{23}, s_{31} they abut.

In circumnavigating the 6π-singularity $s \in M$ clockwise, one must visit the slitted rectangles in one of the two (cyclic) orders s_{12}, s_{23}, s_{31} or s_{12}, s_{31}, s_{23}. The second order is simply the reversal of the first so we deal only with the first. (Both lead to the same discrete datum $[3, 2, 1]$.) Looking at Figure 4, we see that the first order forces the identifications of the vertical sides of $\mathcal{R}$ to be $R_1^+ \leftrightarrow R_3^-$, $R_2^+ \leftrightarrow R_1^-$, $R_3^+ \leftrightarrow R_2^-$. But that means that upon returning to E, the E_i appear in the cyclic order E_3, E_2, E_1 along E. (Indeed, E_3 is followed by E_2 to its right and E_2 is followed by E_1.)

Finally, to uncover the polyband, (still looking at Figure 4) we let L^+ be the broken geodesic obtained by joining s_{12} to s_{23} by a segment in R_2 and s_{23} to s_{31} by a segment in R_3 and s_{31} to s_{12} by a segment in R_1. Cutting $\mathcal{R}$ along L^+ and moving the top pieces below E yields a polyband representing M. It is bounded by L^+ and its rearrangement L^- with discrete datum $[3, 2, 1]$.

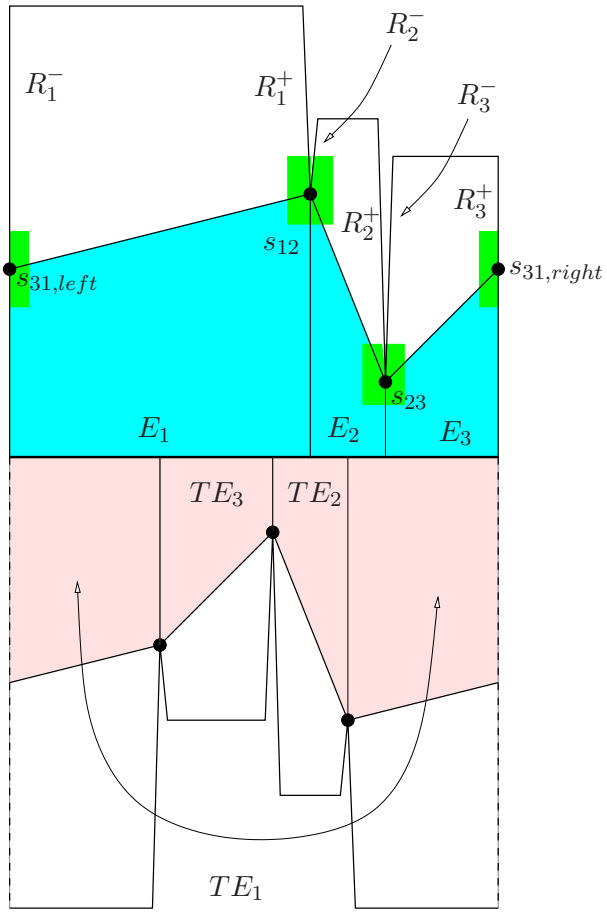

Figure 4: For $M \in \mathcal{H}(2)$, there are three cut points splitting E into E_1, E_2, E_3. The tower of three rectangles above E rearranges into a polyband. The $[3, 2, 1]$ datum is forced because the three slitted rectangles (one presented in two pieces) have to glue so that a neighborhood of the sole singularity with angle 6π is homeomorphic to a disk.

This finishes the proof for $M \in \mathcal{H}(2)$ and we move to the case when $M \in \mathcal{H}(1,1)$, which proceeds along the same lines except that now E is divided into four subarcs E_1, E_2, E_3, E_4. Each of the two singularities corresponds to a pair of the four vertices of $\mathcal{R}$ with angle 2π (named s_{12}, s_{23}, s_{34}, s_{41} according to the rectangles they belong to, see Figure 5).

First observe that such a pair cannot be formed by two vertices that are adjacent (i.e. belong to the same rectangle R_i). Indeed, if that were the case and, say s_{12} and s_{23} were identified in M, then the vertical sides of R_2 above the singularities would be identified as well and so $T(E_2)$ would have to be an arc whose endpoints coincide in M, contradicting $T(E_2)$ being a proper subarc of a simple closed curve E. Therefore, it must be that s_{12} and s_{34} identify to one singularity and s_{23} and s_{41} to the other, as depicted in Figure 5. The identifications of the vertical sides of the tower are then given by $R_1^+ \leftrightarrow R_4^-$, $R_3^+ \leftrightarrow R_2^-$, $R_2^+ \leftrightarrow R_1^-$, $R_4^+ \leftrightarrow$

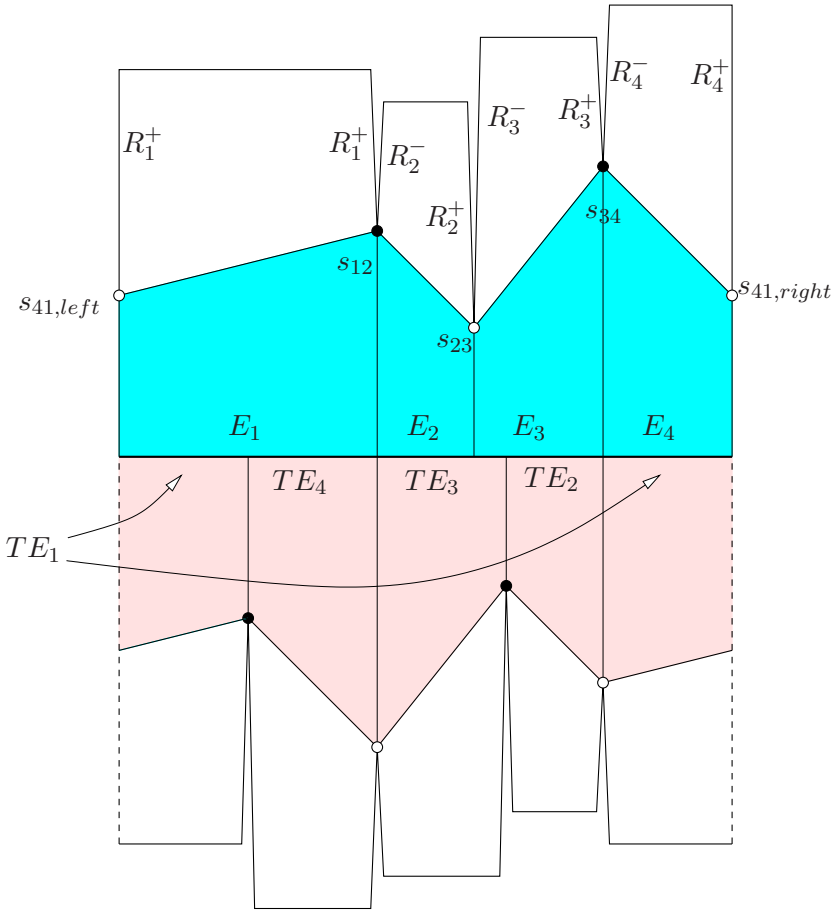

Figure 5: For $M \in \mathcal{H}(1,1)$, the tower of four rectangles above E rearranges into a $[4,3,2,1]$ polyband.

R_3^-. This means that upon returning to E the E_1, E_2, E_3, E_4 appear in the order $T(E_4), T(E_3), T(E_2), T(E_1)$. As before, cutting the tower along the broken line L^+ joining s_{12}, s_{23}, s_{34}, s_{41} leads to a rearrangement into a polyband representing M and with discrete datum $[4,3,2,1]$. □

3 Hyperellipticity

As the first application of Discrete Datum Theorem, we give a geometric reason for the hyperellipticity of all genus two Riemann surfaces — a property usually derived via Riemann-Roch Theorem, [1]. Basically all we have to say is: *Look, the polybands in Figures 4 and 5 are manifestly centrally symmetric.* Let us explain and provide some complex analytic context for this fact.

Recall that the Riemann surface M of the (two-valued) analytic function

$$w = \sqrt{(z-a_1)(z-a_2)\cdots(z-a_n)}$$

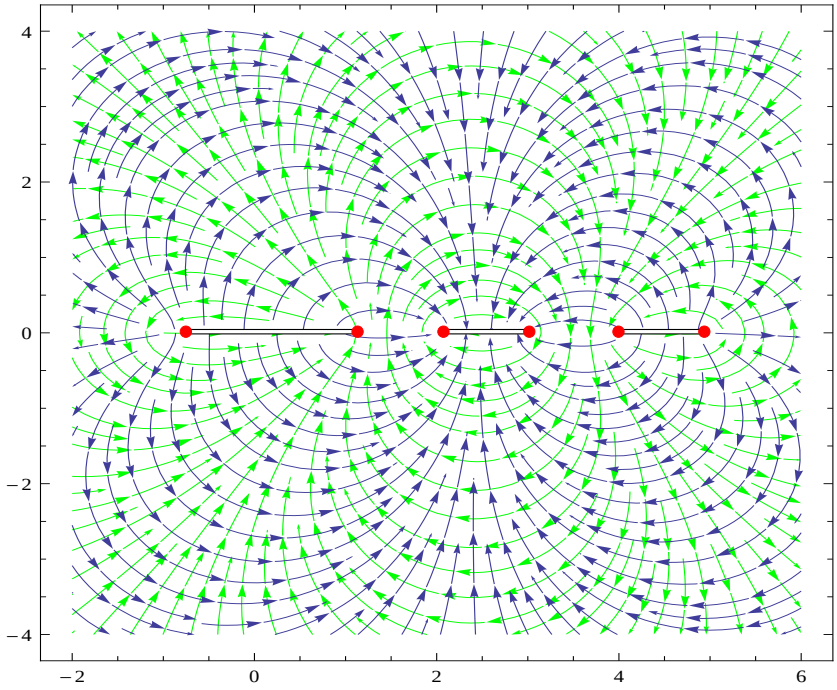

Figure 6: The horizontal and vertical lines of the 1-form $\omega = w^{-1}dz$ on one of the two copies of the triply slitted plane making up the Riemann surface of $w = \sqrt{(z+1)(z-1)(z-2)(z-3)(z-4)(z-5)}$. The real part of ω is $\mathrm{Re}(w^{-1})dx - \mathrm{Im}(w^{-1})dy$ and the darker flowlines are those of the corresponding vectorfield $(\mathrm{Re}(w^{-1}), -\mathrm{Im}(w^{-1}))$. The lighter flowlines similarly correspond to the imaginary part of ω. (Here x and y are the standard coordinates in the depicted z-plane, not the polyband $\mathcal{A}$.)

is conformally equivalent to the Riemann sphere when $n = 1, 2$ and to the complex torus (a quotient of $\mathbb{C}$ by a lattice) if $n = 3, 4$. In the latter case, M is called an *elliptic curve*. The *hyperelliptic curves* are the Riemann surfaces obtained by taking $n > 4$. They are of the smallest genus $g = 2$ for $n = 5, 6$. An abstract Riemann surface M is *hyperelliptic* iff it is conformally equivalent to a hyperelliptic curve, and this is characterized by existence of a conformal involution η with exactly $2g + 2$ fixed points (which are called *Weierstrass points*). Indeed, if such involution η exists, then the quotient M/η is equivalent to the Riemann sphere[4] and the inverse of the natural factor map $\pi : M \to M/\eta$ is essentially the square root function above, with the action of η corresponding to the choice of sign.

To connect with our development, an abstract Riemann surface M can be turned into a translation surface by fixing a holomorphic one form[5] ω on M and

[4] As can be seen by using Riemann-Hurwitz Formula.

[5] Such forms correspond to incompressible irrotational flows on M. One can be usually constructed by hand in any given example (say dz/w in ours) and its a priori existence is *clear* to a physicist. Mathematicians construct them from suitable harmonic functions obtained either as

letting its real and imaginary parts play the roles of the coordinate forms dx and dy (so ω corresponds to $dz = dx + idy$ in the $M = P/\sim$ or $M = \mathcal{A}/\sim$ presentations). Against this backdrop, note that, due to $1, 2, 3, \ldots$ and $\ldots, 3, 2, 1$ being *flips* of each other, any polyband $\mathcal{A}$ with datum $[3, 2, 1]$ or $[4, 3, 2, 1]$ is left invariant under an isometry of the infinite cylinder $\mathcal{S}/\sim$ that rotates it by 180^o about a suitable point, i.e., a mapping given by $(x, y) \mapsto (-x + a, -y + b)$ where x is mod 1 and the parameters a, b are picked so that each segment of L^+ goes to the corresponding segment of L^-. (For the polybands constructed in the proof of Theorem 1 and depicted in Figures 4 and 5, $b = 0$ and a is easy to guess.) We refer to this isometry as the *central symmetry* of $\mathcal{A}$ — although, it has two fixed points: $(a/2, b/2)$ and $(a/2 + 1/2, b/2)$.

The central symmetry respects the boundary identifications in $\mathcal{A}$ that glue it into the surface M and thus induces an isometry $\eta : M \to M$, called the *hyperelliptic involution*, that has exactly 6 fixed points: the two in the interior of the polyband $\mathcal{A}$, one at the center of each side, and the singularity if $M \in \mathcal{H}(2)$. (For $M \in \mathcal{H}(1, 1)$, the two singularities are interchanged.) Viewed on the original Riemann surface, η is conformal — manifestly so away from the singularities but also there (if only because isolated singularities of conformal maps are removable). We established the following classical result:

Corollary 1 (Hyperellipticity)**.** *Any Riemann surface M of genus $g = 2$ is hyperelliptic: it admits a conformal involution $\eta : M \to M$ with six fixed points.*

Before moving on, let us offer the following visually appealing presentation of any $M \in \mathcal{H}(2)$ illustrated by Figure 7.

Theorem 2 (Stamped Torus)**.** *Any $M \in \mathcal{H}(2)$ is isometric to the translation surface obtained by identifying the opposite sides of a parallelogram (perhaps degenerate) in a flat torus (with the interior of the parallelogram removed).*

Proof: By the Discrete Datum Theorem, we may suppose that M is obtained from a polyband construction. First assume that L^+ is not straight (i.e. not all of its segments have the same direction). For each vertex of L^+, consider the (possibly degenerate) triangle spanned by this vertex and the adjacent vertices. One of the triangles has to be non-degenerate and have interior above the polyband — as otherwise L^+ would be convex and thus straight. We may as well suppose that the two sides of this triangle Δ^+ are L_2^+ and L_3^+ (as in Figure 7). By adjoining Δ^+ and its symmetric counterpart $\eta(\Delta^+)$ to the polyband we get a new polyband with the discrete datum $[1, 2]$, which yields a flat torus. The desired parallelogram is obtained by identifying Δ^+ and $\eta(\Delta^+)$ along their edges that are not in $L^\pm$. In the case when L^+ is straight (and thus horizontal), a degenerate parallelogram $L_2^+ \cup L_3^+ = L_3^- \cup L_2^-$ can be used. $\square$

limits of subharmonic functions or as minimizers of a Dirichlet integral, see [1].

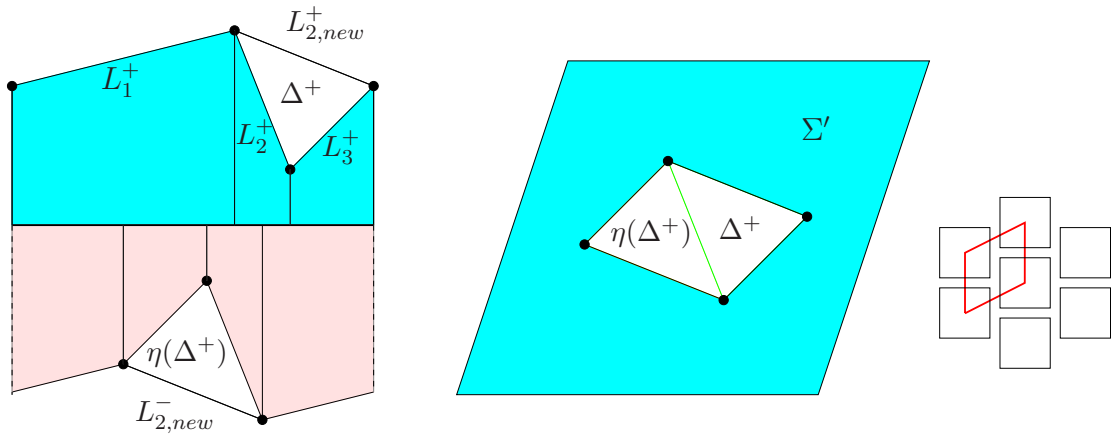

Figure 7: Any $M \in \mathcal{H}(2)$ (left) arises from a flat torus (center) with a parallelogram removed ("stamped out"). Generally (right), the removed parallelogram need not fit into any fundamental parallelogram.

The situation depicted on the right of Figure 7 serves as a warning that some $M \in \mathcal{H}(2)$ cannot be presented as a "big" parallelogram with a "small" parallelogram stamped out (as it happened in the middle of Figure 7).

4 McMullen's Theorem

We turn to our main objective, which is the following restatement of the key combinatorial result in [6] (Theorem 7.4 lumped together with a much easier Theorem 7.3). It implies that any genus two translation surface can be constructed from two slitted parallelograms in a way suggested by Figure 1. Observe that the depicted surface is in $\mathcal{H}(1,1)$. To get a surface in $\mathcal{H}(2)$ one of the slits has to start and end at the same point of the torus.

Theorem 3 (McMullen)**.** *Any translation surface M of genus $g = 2$ contains a saddle connection J such that $\eta(J) \neq J$ (where η is the hyperelliptic involution). The surface M splits along $J \cup \eta(J)$ into a connected sum of two tori. Moreover, given a (maximal) open cylinder C such J can be found so that neither J nor $\eta(J)$ cross ∂C (although they may be contained in ∂C or have endpoints in ∂C).*

Proof: Given a genus $g = 2$ surface M and a cylinder C, we can instantiate the proof of the Discrete Datum Theorem with E being the equator of C to present M via the polyband construction so that C is the maximal horizontal cylinder in the polyband $\mathcal{A}$ — the shaded region in Figures 9 and 10.

We start with the easier case when $M \in \mathcal{H}(2)$. As in the previous argument, we first assume that L^+ is not straight and consider the triangles spanned by each vertex of L^+ together with the two adjacent vertices. Again, one such triangle, call it Δ^+, has to be non-degenerate and contained in $\mathcal{A}$ (see Figure 8). The desired

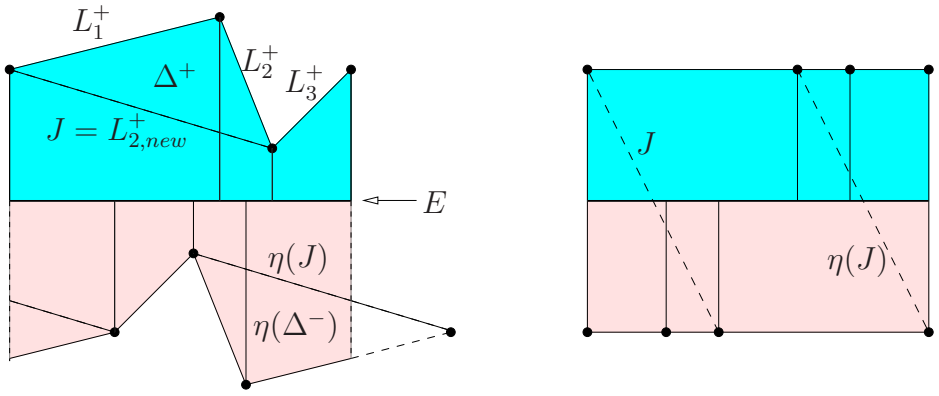

Figure 8: The construction of J for $M \in \mathcal{H}(2)$; the degenerate case on the right.

J is the lower side of Δ^+ (the side not in L^+). Indeed, cut away from $\mathcal{A}$ along $J \cup \eta(J)$, Δ^+ and $\eta(\Delta^+)$ naturally identify to form a torus and $\mathcal{A} \setminus (\Delta^+ \cup \eta(\Delta^+))$ is a new polyband with the discrete datum $[2, 1]$, yielding a torus as well. For J when L^+ is straight, see Figure 8.

It remains to deal with the case when $M \in \mathcal{H}(1, 1)$. The situation is a bit more complicated by virtue of L^+ containing four segments. L^+ is a graph of a function over E and we may well assume that s_{41} is the minimum, the lowest point of L^+. The segment L_1^+ must then go *up*, i.e., have a non-negative slope. Subsequent segments L_2^+, L_3^+ can go *up* or *down* and L_4^+ has to go *down*, i.e., have a non-positive slope. Below we consider the four possibilities for the slopes of $L_1^+, L_2^+, L_3^+, L_4^+$: *up,up,up,down*, *up,down,down,down*, *up,up,down,down*, and *up,down,up,down*. (These are not exactly mutually exclusive because some slopes may be zero.) We first restrict attention to the "non-degenerate" situation when the minimum on L^+ is attained at the sole location s_{41}.

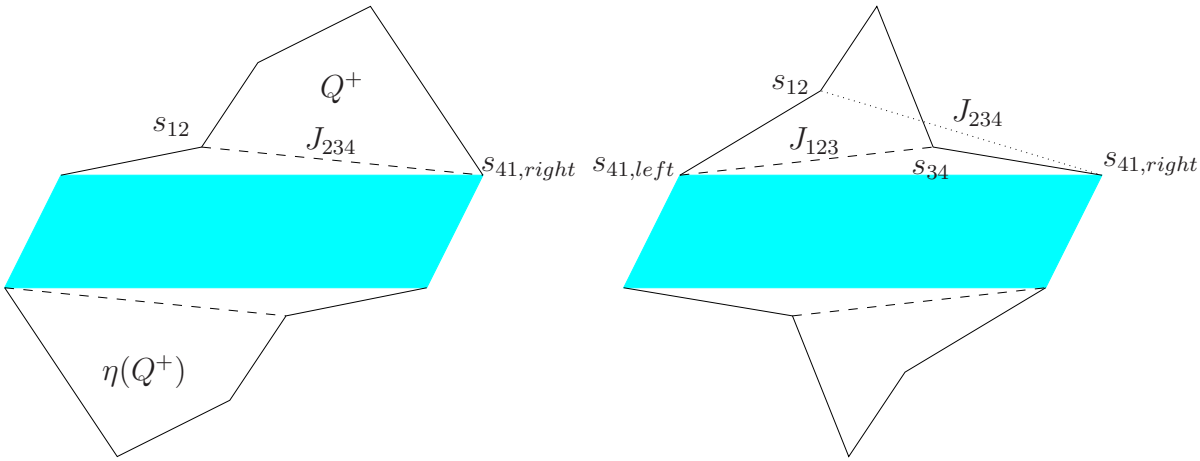

Figure 9: *up,up,up,down* and *up,up,down,down* (non-degenerate cases).

up,up,up,down: Let $J = J_{234}$ connect s_{12} to the "rightmost" point of L^+, $s_{41,right}$

in Figure 9. Observe that the segments J, L_2^+, L_3^+, L_4^+ bound a quadrilateral Q^+. Q^+ and $\eta(Q^+)$ glue (along J and $\eta(J)$) to form a hexagon, which identifies to a torus. What remains of the polyband $\mathcal{A}$ has discrete datum $[2, 1]$ so also forms a torus.

up,down,down,down: This case is (vertical) axis-symmetric to the previous one.

up,up,down,down: Consider J_{234} as in the first case and its symmetric counterpart J_{123} connecting the leftmost point $s_{41,left}$ of L_4^+ to s_{34}, see Figure 9. $J = J_{234}$ is as desired unless it is not entirely contained in the polyband $\mathcal{A}$, which is when s_{34} is below J_{234}. Likewise, $J = J_{123}$ works unless s_{12} is below J_{123}. It is impossible for s_{12} and s_{23} to be both "below".

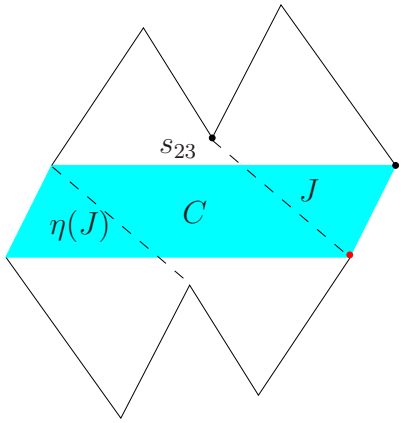

Figure 10: *up,down,up,down* (non-degenerate case): an "easy" J could be found if it were allowed to cross ∂C.

up,down,up,down: Now s_{23} is a local minimum on L^+ (but it is not in ∂C by our temporary non-degeneracy assumption). It is really easy to find a suitable J that crosses ∂C; see Figure 10. For J that does not cross ∂C we have to work a bit harder.

Let K^+ be the triangle in $\mathcal{A}$ with L_3^+ and L_4^+ for its two sides. Upon identifying a pair of parallel sides in $K^+ \cup \eta(K^+)$ we get a cylinder $K \subset M$. Consider the oriented half-line D originating from $s_{41,left}$ and passing through s_{23}. The portion of D in the cylinder K cuts K into a parallelogram. The union of this parallelogram and the triangle with vertices $s_{41,left}, s_{23}, s_{41,right}$ forms a trapezoid (see Figure 11). Note that the side opposite to the $s_{41,left}, s_{41,right}$-side in the trapezoid must contain a point that represents a singularity. Let J be the segment in the trapezoid connecting that point to $s_{41,left}$. Note that $\eta(J) \neq J$ (if only because, presented[6] in $\mathcal{A}$, $\eta(J)$ ends at $\eta(s_{41,right})$ which is not in J). From $\eta(J) \neq J$, it already follows that M cut along $\gamma := \eta(J) \cup J$ disassociates into two slitted tori (cf. Theorem 7.3 in [6]). Indeed, since η acts on the first homology $H_1(M, \mathbb{Z})$ by $-\mathrm{Id}$ and $\eta(\gamma) = \gamma$, γ is a null homologous loop and thus cuts M into two

[6]We abuse the notation η: in the context of $\mathcal{A}$, η is the *obvious central symmetry*.

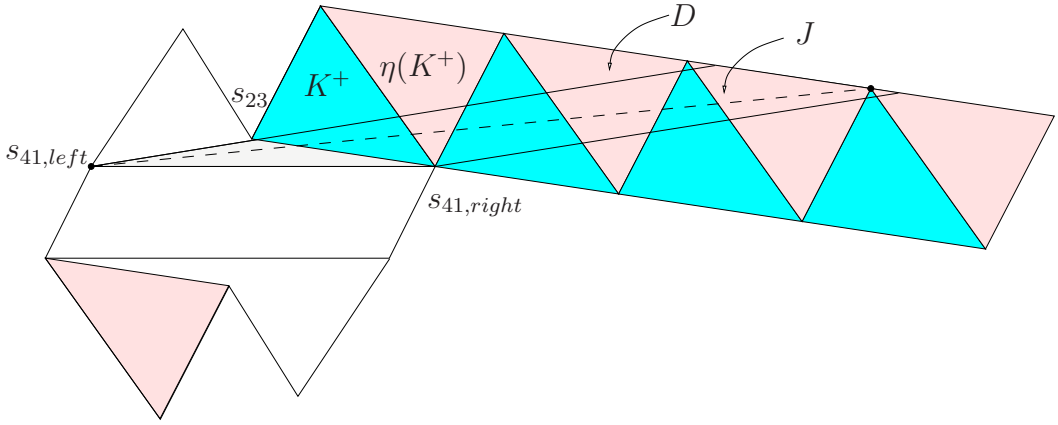

Figure 11: *up,down,up,down* (non-degenerate case): K^+ and $\eta(K^+)$ form a cylinder, which is shown "unfolded" to unveil the trapezoid inside which J is found.

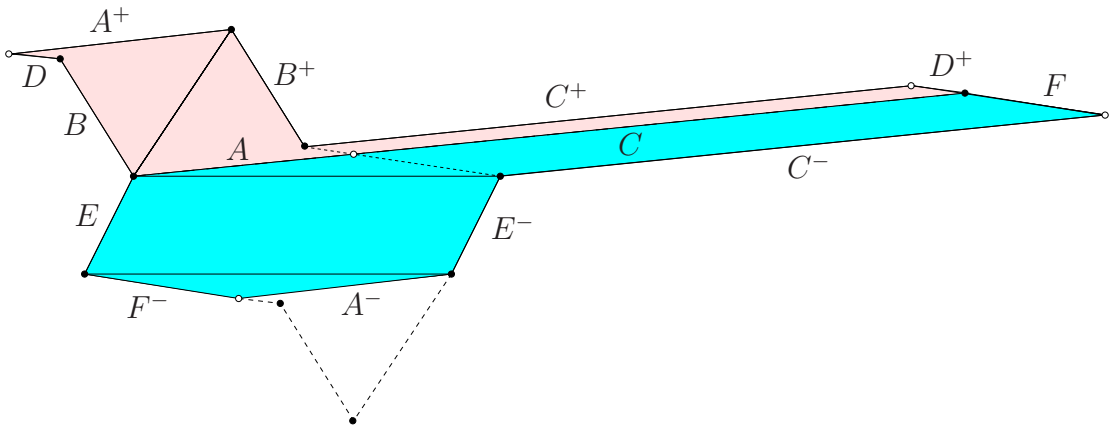

Figure 12: J and $\eta(J)$ cut M into two tori (presented by the two shaded hexagons).

subsurfaces of lower genus. For concreteness, Figure 12 identifies those two tori explicitly.

The proof is complete save for the degenerate cases when s_{41} is not the only vertex of L^+ in ∂C. These are all easy and taken care of in Figure 13.

□

References

[1] H. M. Farkas and I. Kra. *Riemann surfaces*, volume 71 of *Graduate Texts in Mathematics*. Springer-Verlag, New York, second edition, 1992.

[2] P. Hubert, E. Lanneau, and M. Möller. $\mathrm{GL}_2^+(\mathbb{R})$-orbit closures via topological splittings. In *Geometry of Riemann surfaces and their moduli spaces*, volume 14 of *Surveys in differential geometry*, pages 145–169. Int. Press, Somerville, MA, 2009.

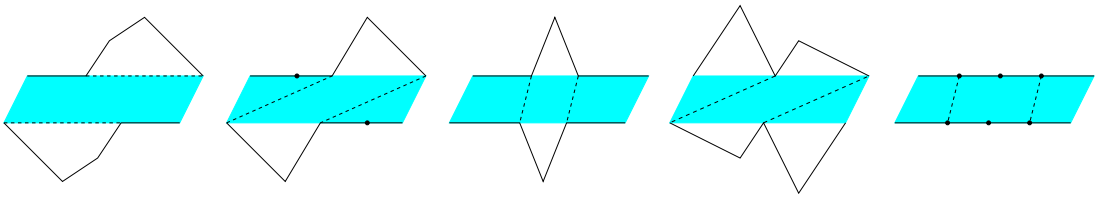

Figure 13: Degenerate cases with 3, 2, and all 4 vertices of L^+ in ∂C. (The second and third pictures are essentially the same.)

[3] S. Kerckhoff, H. Masur, and J. Smillie. Ergodicity of billiard flows and quadratic differentials. *Ann. of Math. (2)*, 124(2):293–311, 1986.

[4] H. Masur. Closed trajectories for quadratic differentials with an application to billiards. *Duke Math. J.*, 53(2):307–314, 1986.

[5] H. Masur and S. Tabachnikov. Chapter 13: Rational billiards and flat structures. In B. Hasselblatt and A. Katok, editors, *Handbook of Dynamical Systems*, volume 1, Part 1A, pages 1015 – 1089. Elsevier Science, 2002.

[6] C.T. McMullen. Dynamics of $SL_2(\mathbb{R})$ over moduli space of genus two. *Ann. of Math.*, 165:397–456, 2007.

[7] J. Smillie. The dynamics of billiard flows in rational polygons. In *Dynamical systems, ergodic theory and applications*, volume 100 of *Encyclopaedia of Mathematical Sciences*, pages 360–382. Springer, Berlin, 2000.

[8] W. Veech. Gauss measures for transformations on the space of interval exchange maps. *Ann. of Math. (2)*, 115(1):201–242, 1982.

[9] Y. Vorobets. Periodic geodesics on translation surfaces. Preprint, arXiv:math/0307249v1, 2003.

[10] A. Zorich. Flat surfaces. In *Frontiers in number theory, physics, and geometry. I*, pages 437–583. Springer, Berlin, 2006.